Article

Cell Reports

Cell Cycle Inhibitor Whi5 Records Environmental Information to Coordinate Growth and Division in Yeast

Graphical Abstract

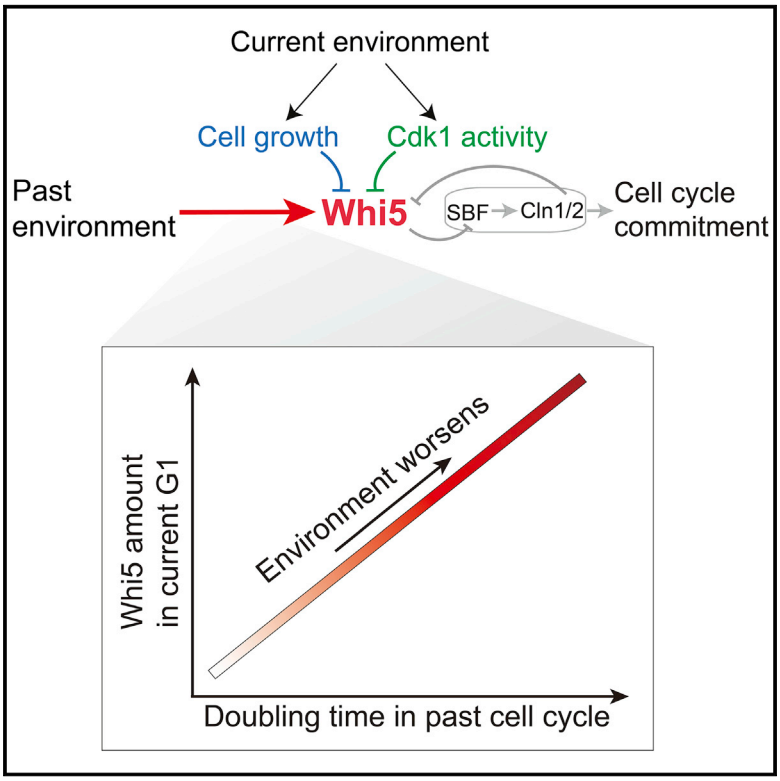

Highlights

- The cell cycle inhibitor Whi5 remembers the cell's growth rate in the past cycle
- Whi5 plays an important role in the homeostasis of cell growth and division
- The synthesis rate of Whi5 is independent of the environment and cell growth rate
- Cells use past and current environmental information to control cell cycle entry

Authors

Yimiao Qu, Jun Jiang, Xiang Liu, Ping Wei, Xiaojing Yang, Chao Tang

Correspondence

xiaojing_yang@pku.edu.cn (X.Y.), tangc@pku.edu.cn (C.T.)

In Brief

Qu et al. find that the level of the cell cycle inhibitor Whi5 is proportional to the doubling time of the past cell cycle across a variety of nutrient and stress conditions. Thus, both past and current environmental information is utilized in coordinating cell growth and division.

Qu et al., 2019, Cell Reports *29*, 987–994
October 22, 2019
https://doi.org/10.1016/j.celrep.2019.09.030

CellPress

Cell Reports
Article

Cell Cycle Inhibitor Whi5 Records Environmental Information to Coordinate Growth and Division in Yeast

Yimiao Qu,[1,4] Jun Jiang,[1,4] Xiang Liu,[1,4] Ping Wei,[1,2] Xiaojing Yang,[1,*] and Chao Tang[1,3,5,*]
[1]Center for Quantitative Biology and Peking-Tsinghua Center for Life Sciences, Academy for Advanced Interdisciplinary Studies, Peking University, Beijing 100871, China
[2]The MOE Key Laboratory of Cell Proliferation and Differentiation, School of Life Sciences, Peking University, Beijing 100871, China
[3]School of Physics, Peking University, Beijing 100871, China
[4]These authors contributed equally
[5]Lead Contact
*Correspondence: xiaojing_yang@pku.edu.cn (X.Y.), tangc@pku.edu.cn (C.T.)
https://doi.org/10.1016/j.celrep.2019.09.030

SUMMARY

Proliferating cells need to evaluate the environment to determine the optimal timing for cell cycle entry. However, how this is achieved is not well understood. Here, we show that, in budding yeast, the G1 inhibitor Whi5 is a key environmental indicator and plays a crucial role in coordinating cell growth and division. We found that, under a variety of nutrient and stress conditions, Whi5 amount in G1 is proportional to the cell's doubling time in the environment, which in turn influences the timing for the next cell cycle entry. In addition, the coordination between division and environment is further fine-tuned in G1 by environmentally dependent growth rate, G1 cyclin-Cdk1 contribution, and Whi5 threshold at the start. Our results show that the cell stores the past environmental information in Whi5, which works together with other mechanisms sensing the current environmental condition to achieve an adaptive cellular decision making process.

INTRODUCTION

Coordination of the cell cycle with environmental conditions is a classic example of biological adaptation, which entails the cell-making decisions based on its assessment of the environment (Johnson and Skotheim, 2013; Jorgensen and Tyers, 2004). In budding yeast, the decision to divide is made in G1 phase and the commitment to cell cycle (Start; Hartwell et al., 1974) is governed by a biochemical switch composed of a double-negative feedback loop between the inhibitor Whi5 and the G1-cyclin Cln1/2 (Bean et al., 2006; Costanzo et al., 2004; de Bruin et al., 2004; Figure 1A). In early G1, Whi5 forms a complex with the transcription factor SBF (Swi4–Swi6 cell cycle box binding factor), inhibiting the transcription of ~200 G1/S genes (Bean et al., 2006; Costanzo et al., 2004).

Several mechanisms have been proposed to coordinate the Start transition with the environmental condition. First, Cln3-Cdk1 phosphorylates Whi5, leading to its nuclear export (de Bruin et al., 2004). Cln3 has long been thought to act as a nutrient sensor; its transcription, translation, and localization were all reported to be regulated by environmental signals (Hall et al., 1998; Polymenis and Schmidt, 1997; Shi and Tu, 2013). The turnover rates of both its mRNA and the protein are extremely fast (~min; Arava et al., 2003; Cross and Blake, 1993; McInerny et al., 1997; Tyers et al., 1992; Yaglom et al., 1995; Cai and Futcher, 2013), enabling a fast response to changes in environmental conditions. Recently, Cln3 was found to act on Whi5 through an integration mechanism that integrates the Cln3-Cdk1 activity over a time window between 3 and 12 min (Chandler-Brown et al., 2017; Liu et al., 2015). The same study also hinted the role of Whi5 in coordinating Start transition with the nutrient conditions, but the underlying mechanism is still unclear. Second, it has been reported that the dilution of nuclear Whi5 concentration by cell growth plays an important role in promoting Start in ethanol, a poor nutrient (Schmoller et al., 2015). On the other hand, a recent study found no evidence for Whi5 nuclear concentration dilution during G1 for cells grown in glucose and glycerol and instead found that the concentration of SBF positively correlated with cell size in G1 and that both SBF and Cln1 levels were upregulated in the poor nutrient glycerol, suggesting yet another mechanism to inactivate Whi5 by stoichiometry (Dorsey et al., 2018). Furthermore, Ras/cyclic AMP (cAMP)/protein kinase A (PKA) signaling pathway has also been proposed to contribute to the coordination of Start transition with the environment via Swi4 phosphorylation to modulate the expression of Cln1/2 (Amigoni et al., 2015; Baroni et al., 1994; Tokiwa et al., 1994).

The timing of Start sets the length of the G1 phase, which plays a critical role in coordinating growth with division. The G1 length is determined by three factors: the initial value of the nuclear Whi5 concentration; the rate at which this concentration decreases; and the threshold concentration for Start. The first two mechanisms—nuclear exclusion by CDK phosphorylation and dilution via growth—reduce the nuclear concentration of Whi5, and the third mechanism—increasing Whi5's inhibiting target SBF—effectively raises the threshold concentration of nuclear Whi5 at Start. Although these regulations play crucial roles to trigger Start, another important factor is the initial nuclear

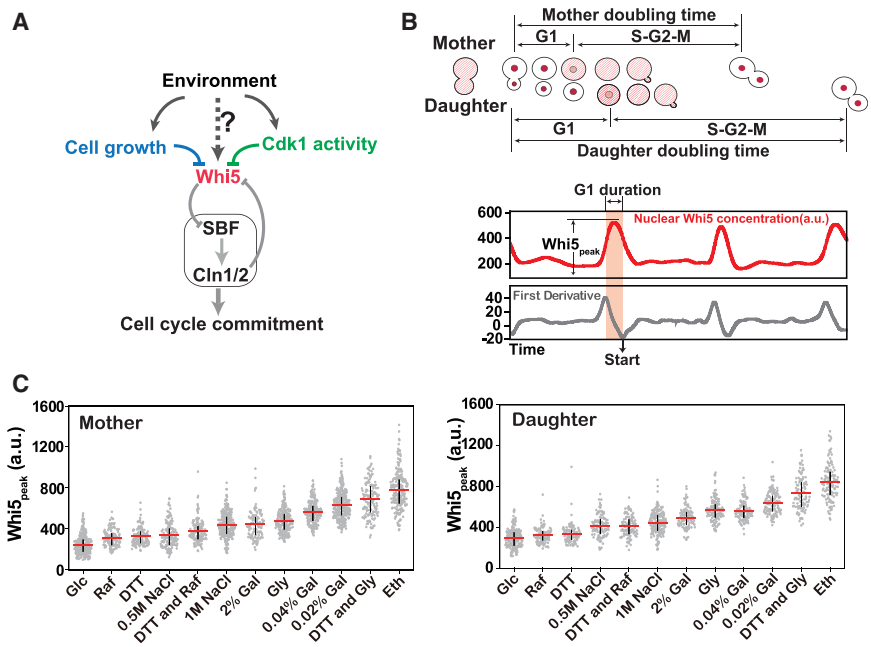

Figure 1. Whi5 Level in G1 Reflects the Environmental Condition

(A) Schematic of the Start regulatory network. The inhibitor Whi5, the transcription activator SBF, and the cyclin Cln1/2 form a double-negative feedback loop. Cell cycle entry is blocked by Whi5 via repression of the master transcription factor SBF for G1/S transition. Nuclear Whi5 concentration decreases as a result of cell growth and G1 cyclin-CDK activity. Start is triggered irreversibly when the feedback loop overcomes Whi5 repression.

(B) Cartoon (upper) and sample (lower) traces of Whi5 dynamics throughout the cell cycle. The nuclear Whi5 concentration ($Whi5_{nuc}$), its peak level ($Whi5_{peak}$), the doubling time, and the G1 duration were measured in single cells. The G1 duration was defined as the time between the maximum and minimum of the first derivative of the $Whi5_{nuc}$ profile.

(C) Peak concentration of nuclear Whi5 in G1 under different growth conditions at steady state for mother (left panel) and daughter (right panel) cells. The applied conditions are indicated on the horizontal axis–DTT: 0.5 mM DTT; Eth, 2% ethanol; Gal, 2% galactose; Glc, 2% glucose; Gly, 2% glycerol; NaCl, 1 M NaCl; Raf, 2% raffinose. Mother cells, n = 309, 127, 140, 154, 137, 269, 118, 231, 215, 288, 144, and 212 (from left to right). Daughter cells, n = 188, 108, 117, 195, 114, 113, 138, 112, 113, 138, 109, and 123 (from left to right). Red bars indicate the mean and black bars indicate 25% and 75% of the data.

concentration of Whi5 in G1. It is known that, under the same nutrient condition, cells with higher Whi5 level have longer G1 length (Costanzo et al., 2004; de Bruin et al., 2004; Liu et al., 2015). However, it is not clear how Whi5 level changes across different nutrient and environmental conditions and, if so, how Whi5 level is coupled to the environment and what is the implication to Start regulation. Here, we address these questions by simultaneously monitoring Whi5 dynamics, cell size, doubling time, and the G1 duration in single cells, together with studies of Whi5 transcription and degradation, in a variety of nutrient and stress conditions. Our work revealed a principle of how cells use Whi5 to evaluate the environmental conditions and determine the time of Start accordingly. In combination with a mathematical model, we further investigated and explained how cells integrate different mechanisms of Start transition in an environmentally dependent manner.

RESULTS

Nuclear Whi5 Level in G1 Varies Significantly across Different Environmental and Stress Conditions

We first measured the level of nuclear Whi5 in different environments characterized by various nutrients, stresses, and combinations of the two. To maintain a constant environmental condition, we employed a microfluidics system (Figure S1A), and all measurements were conducted after the cells had fully adapted to the given conditions. We fused endogenous Whi5 with tdTomato at the C terminus and monitored the spatiotemporal dynamics of Whi5 in single cells. Additionally, we tracked the cell size, doubling time (T_D), and the G1 duration, defined as the time during which Whi5 is sequestered in the nucleus (Figures 1B and S1B–S1H).

The maximum concentration of Whi5 in the nucleus during G1 (referred to as $Whi5_{peak}$) varied significantly in different environments (Figure 1C; Data S1). No changes in the coefficient of variation (CV) of $Whi5_{peak}$ were found as the environment varied, suggesting a tight regulation of nuclear Whi5 level under all conditions investigated (see also Data S2). Generally, nuclear Whi5 level increased as the environmental condition worsened: $Whi5_{peak}$ increased with decreased nutrient level and quality and with increased stress level (NaCl concentration; Figure 1C). Furthermore, we found that $Whi5_{peak}$ in poor nutrients was further elevated by stress (DTT; Figure 1C), suggesting a mechanism for integrating environmental conditions at the Whi5 protein level. Because the cell size is typically smaller in worse conditions, we tested that the increase of Whi5 concentration was not just due to the change of cell size across conditions (Figures S1H and S1I; Data S2).

The Amount of Whi5 in G1 Is Proportional to the Doubling Time across Different Environmental Conditions

We then looked at the dependency of the total amount of Whi5 in G1, $Whi5_{tot}$, on the quantity that best reflects the environmental conditions, i.e., the doubling time. We found that $Whi5_{tot}$ was linearly proportional to the doubling time in all conditions we tested (Figure 2A). The amount of a protein is determined by its synthesis rate and removal rate. We measured Whi5 degradation during the cell cycle under various conditions, and no degradation was observed (Figures 2B and S2A), implying that the removal of Whi5 is solely due to cell division. Without degradation,

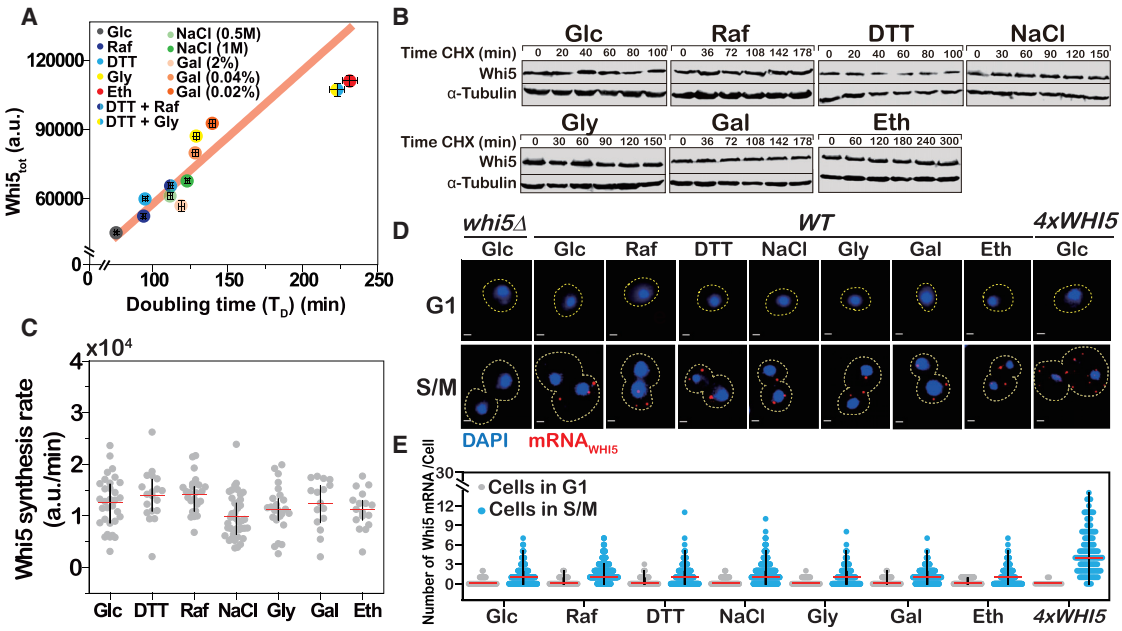

Figure 2. Whi5 Level in G1 Is Proportional to the Doubling Time across Conditions

(A) Average Whi5 amount in early G1 versus the average doubling time under the indicated conditions. The average doubling time represents the state of the entire cell population, including data from both mother and daughter cells. The red line is a linear fit with $R^2 = 0.99$. Bars, mean ± SEM. Numbers of cells are the same as in Figure 1C.

(B) Cycloheximide chase analysis of Whi5 degradation under various conditions. Immunoblotting results show Whi5 protein levels after treatment with cycloheximide for the indicated times (time CHX). α-tubulin was used as a loading control.

(C) The estimated Whi5 synthesis rate under the indicated condition. Each dot represents a single cell measurement. Red bars indicate the mean, and black bars indicate 25% and 75% of the data.

(D) Representative smFISH fluorescent images of cells in G1 phase (upper) and cells in S-M phase (lower) of the cell cycle under the indicated conditions. Each red dot in the fluorescent image represents a single WHI5 mRNA. We measured the mRNA levels in WHI5-deleted (*whi5Δ*) cells as a negative control. We also compared cells containing 4 copies of WHI5 gene (4 × WHI5) with *WT* cells, and the 4 × WHI5 cells exhibited markedly increased WHI5 mRNA levels. Scale bars, 2 μm.

(E) Numbers of WHI5 mRNAs in G1 cells (gray dots) and S/M cells (blue dots) cultured in different media: Glc (n = 138 and 649); Raf (n = 202 and 890); DTT (n = 229 and 731); NaCl (n = 260 and 873); Gly (n = 131 and 440); Gal (n = 211 and 725); and Eth (n = 276 and 799). Cells with 4 copies of WHI5 gene (4 × WHI5) are also shown for comparison (n = 19 and 159). Red bars indicate the median; black bars indicate 25% and 75% of the data (see Data S3 for more statistics). Note that the median WHI5 mRNA copy number in G1 cells is zero under all conditions and the median in S/M cells is one under all conditions except in the 4 × WHI5 cells.

the amount of Whi5 at the end of a cell cycle (before division) is simply the amount of Whi5 at the beginning of the cell cycle plus the total synthesis during the cell cycle, which is $Whi5_n^{end} = Whi5_n^{begin} + \alpha \cdot T_D$, where n denotes the n^{th} cell cycle, α the average synthesis rate, and T_D the doubling time. At cell division, the amount of Whi5 is then distributed to two cells: $Whi5_{n+1}^{begin} = (1/2)Whi5_n^{end}$. In the steady state, we have $Whi5_n^{begin} = (1/2)Whi5_n^{end} = (1/2)(Whi5_n^{begin} + \alpha \cdot T_D)$, which gives $Whi5_n^{begin} = \alpha \cdot T_D$. The observed linear relationship between $Whi5_{tot}$ (a measure of $Whi5^{begin}$) and T_D (Figure 2A) would imply a synthesis rate α independent of the environmental conditions. We next estimated the synthesis rate of Whi5 in single cells, using the time profile of Whi5 (see also STAR Methods), under various conditions (Figures 2C and S2B). Indeed, Whi5 synthesis rate is approximately the same across all conditions we tested.

Because ploidy is an important determinant of protein synthesis, we introduced different gene copy numbers of WHI5, measured $Whi5_{tot}$ and T_D values, and then calculated Whi5 synthesis rate with the formula $\alpha = (Whi5_{tot}/T_D)$. The α value was found to be linearly correlated with the WHI5 copy number ($R^2 = 0.9$; Figure S2C). Thus, the synthesis rate of Whi5 depended on the gene copy number, but not on the environment.

The Amount of WHI5 mRNA Is Independent of Environmental Conditions

To further test the hypothesis that the synthesis rate of Whi5 is independent of the environmental conditions, we measured the amount of WHI5 mRNA in single cells under various conditions using single-molecule fluorescent *in situ* hybridization (smFISH). No apparent environmental dependence was observed (Figures 2D and 2E; Data S3). It is worth noting that the number of WHI5 mRNAs was significantly higher in budded cells (S/M phases) than in cells without a bud (G1 phase), suggesting that WHI5 transcription mainly occurs in S/M phases, but not in G1 (Figures 2D and 2E), a result consistent with previous studies (Pramila et al., 2006; Schmoller et al., 2015).

To see whether the regulation of Whi5 expression across environmental conditions was due to some global gene-regulation program, we selected 87 genes, including representative genes in cell cycle, metabolism, protein synthesis, and some other

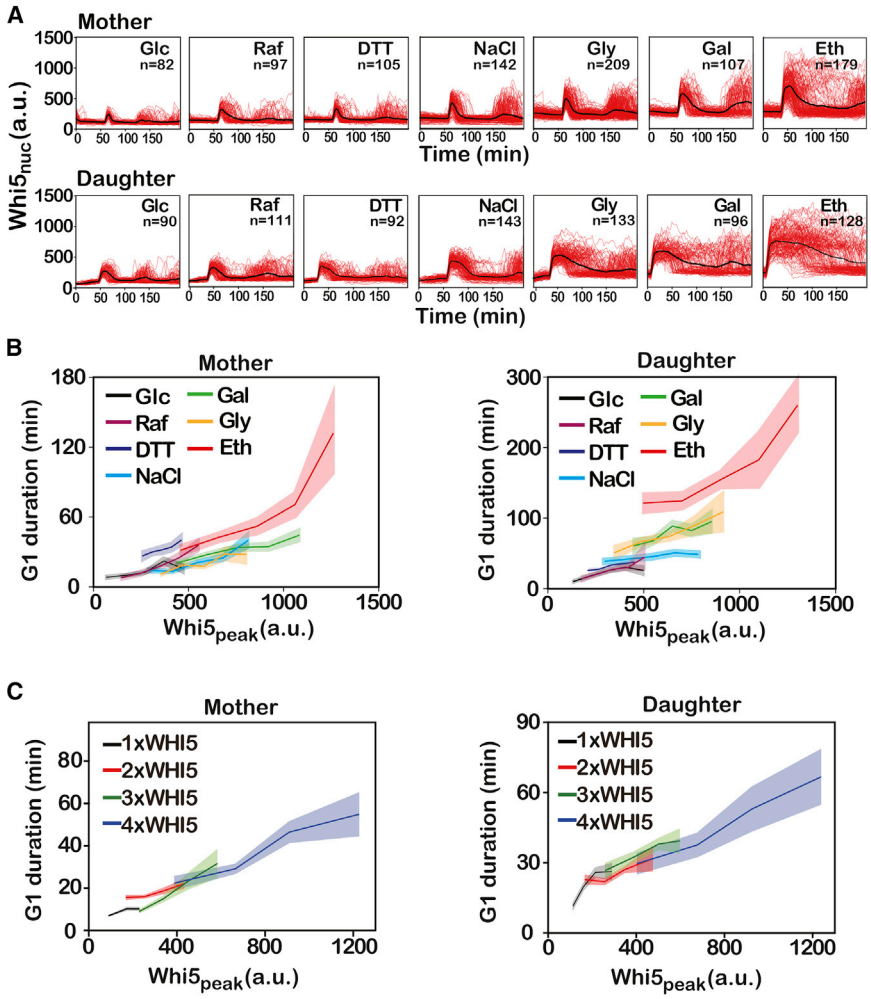

Figure 3. The G1 Duration Is Positively Correlated with Whi5 Level within and across Conditions

(A) Single-cell traces of the nuclear Whi5 level $Whi5_{nuc}$ in mother (upper panel) and daughter (lower panel) cells under various conditions (red curves). Black curves are the average $Whi5_{nuc}$.

(B) The G1 duration versus $Whi5_{peak}$ in mother (left) and daughter (right) cells under various conditions. Shade, SEM.

(C) The G1 duration versus $Whi5_{peak}$ in cells with different copy numbers of the WHI5 gene in Glc medium. Mother cells (left), n = 135, 169, 128, and 213; daughter cells (right), n = 114, 124, 102, and 101. Shade, SEM.

randomly selected genes, from the yeast GFP library (Huh et al., 2003) and measured their expression level in the steady state under five conditions using flow cytometry. Comparing with their expression levels in a fast-growing condition (glucose with no stress), most of the genes were downregulated in poorer nutrients and some were upregulated in the stressed condition. Whi5 was the only one among the 87 that consistently exhibited upregulation in all four poorer conditions (Figure S1J; Data S3), indicating a special regulation mechanism across the environmental conditions.

G1 Duration Increases with $Whi5_{peak}$ within and across Conditions

With its synthesis rate independent of the environment and its removal solely dependent on cell division, Whi5 level is a direct measure of the doubling time (or more precisely the doubling time minus the G1 duration), which is the most accurate indicator of the environmental conditions over the timescale of the doubling time. To investigate how cell uses this information of environment to regulate the next cell cycle, we examined the correlation between $Whi5_{peak}$ and the duration of G1 phase in single cells under different conditions. We found that the G1 duration was generally extended as $Whi5_{peak}$ increased under all conditions examined (Figures 3A, 3B, S3A, and S3B). This means that, in poorer conditions (measured by the longer doubling times), a higher $Whi5_{peak}$ would result in a longer G1. In other words, cells in poor conditions have to grow longer in G1 to overcome a higher $Whi5_{peak}$ barrier. This mechanism naturally coordinates growth and division: poor condition → longer doubling time → higher Whi5 level in the cell → longer G1 to assure sufficient growth for the next division.

There Are Also Other Factors Determining G1 Length across Different Conditions

Note that $Whi5_{peak}$ is not the sole determinant of G1 duration. For cells having the same $Whi5_{peak}$ but in different conditions, the ones in poorer condition have longer G1 (Figure 3B). In comparison, we artificially changed the level of $Whi5_{peak}$ by introducing different numbers of WHI5 gene in the cell and examined the correlation between $Whi5_{peak}$ and G1 duration under a fixed condition (Figures 3C and S3C–S3E). Both $Whi5_{peak}$ and the G1 duration increased as the gene copy number increased, and the G1 duration is more or less a single valued function of $Whi5_{peak}$. Although the $Whi5_{peak}$ levels in the 4 × WHI5 cells in a good condition were comparable to that under the poor conditions, the G1 durations were much shorter (Figures 3B and 3C). These observations suggest that there are other environmentally sensitive factors contributing to further tuning the G1 length (Schneider et al., 2004). Indeed, as discussed in the introduction, there are multiple mechanisms in G1 to inactivate Whi5, which all couple to the environmental conditions.

To deconvolute the multiple contributions to trigger Start, we investigated the dynamics of the nuclear Whi5 concentration in detail in single cells under various conditions. Two independent mechanisms are thought to contribute to the decrease in nuclear Whi5 concentration during G1 phase: exclusion from the nucleus due to Cdk1 phosphorylation (de Bruin et al., 2004) and dilution via cell growth (Schmoller et al., 2015; Figure 4A). Based on our

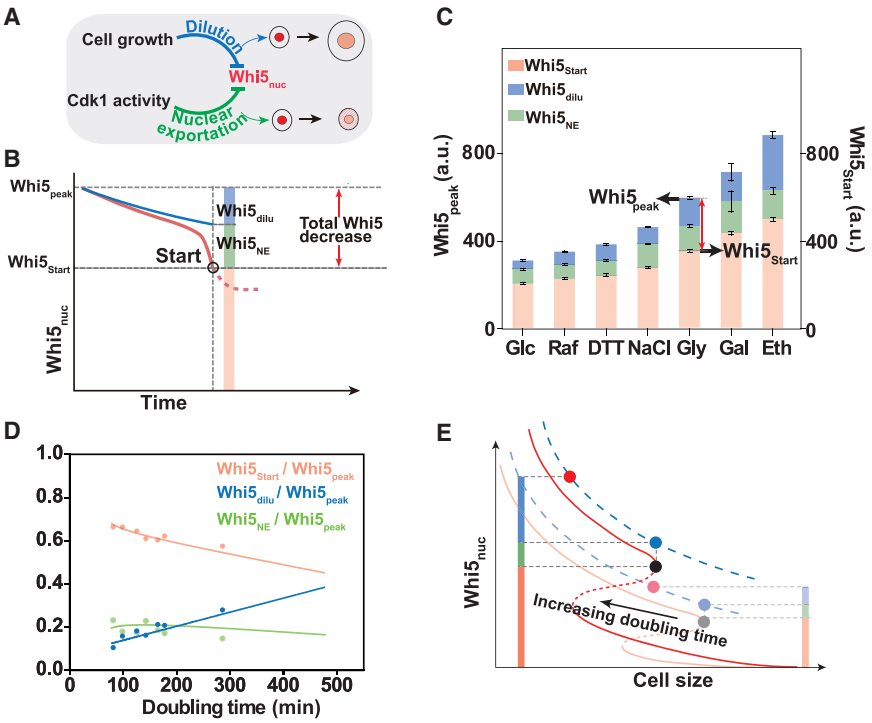

Figure 4. Cells Coordinate Whi5 Dilution, Nuclear Exportation, and Start Threshold to Ensure Adaptive Cell Cycle Start

(A) Schematic representation of the decrease in the nuclear Whi5 concentration ($Whi5_{nuc}$) during G1. This is promoted by both cell growth (dilution) and Cdk1 activity (phosphorylation).

(B) The irreversible G1/S transition begins when the nuclear Whi5 concentration drops below a critical point. The red line represents the observed decrease in Whi5 (actual nuclear concentration). The blue line represents the inferred Whi5 concentration if all Whi5 were kept in the nucleus and the concentration decrease was only due to the growing nuclear volume. The difference between $Whi5_{peak}$ and the blue line is denoted as $Whi5_{dilu}$. The difference between blue line and red line is denoted as $Whi5_{NE}$ ($Whi5_{NE}$ is an inference; $Whi5_{NE} = Whi5_{peak} - Whi5_{Start} - Whi5_{dilu}$). The Start point was defined in Figure 1B.

(C) The nuclear Whi5 concentration at Start ($Whi5_{Start}$), the nuclear Whi5 concentration decrease due to dilution ($Whi5_{dilu}$), and the nuclear Whi5 concentration decrease due to phosphorylation ($Whi5_{phos}$) under various growth conditions. These three quantities add up to the peak Whi5 nuclear concentration ($Whi5_{peak}$). The bars are colored as defined in (B). Data were averaged over many single cells. The error bar is the SD. $Whi5_{peak}$ increases as the conditions worsen, as do $Whi5_{Start}$ and the contribution from dilution.

(D) The same quantities in (C) but normalized by corresponding $Whi5_{peak}$ in each condition and plotted as functions of the doubling time (dots). The solid lines were modeling results.

(E) Schematic representation of the nuclear Whi5 behavior in G1 according to the mathematical model. Red curves represent the nuclear Whi5 concentration as a function of the cell size (note the bistable behavior), and blue dashed lines represent the hypothetical trajectory of nuclear Whi5 concentration due to cell growth dilution only. The differences between the blue and red lines are the effect of Cdk1 phosphorylation. Two sets of lines (dark and light colored) indicate two different environmental conditions. Starting from $Whi5_{peak}$ (red dots), nuclear Whi5 concentration decreases smoothly as the cell grows until it reaches a critical point (black dots) when the Start transition happens.

smFISH experiments, there were essentially no Whi5 protein syntheses in G1 phase (Figures 2D and 2E; Data S3). Thus, we could estimate the contribution of dilution from the observed changes in nuclear volume during G1. As the size of the nucleus in yeast is proportional to the cell size (Jorgensen et al., 2007), we directly used the cell size to calculate the decrease in nuclear Whi5 concentration via dilution, and any additional decrease in nuclear Whi5 concentration would be due to Whi5 nuclear exportation (Figure 4B). We focused on daughter cells here (mother cells exhibited no significant growth during G1; Figure S4B), and it was difficult to accurately measure the change in cell size during G1 phase, especially under good conditions).

We examined the dynamics of nuclear Whi5 concentration during G1 phase in single cells under various conditions and obtained the contributions to nuclear Whi5 concentration decrease from dilution ($Whi5_{dilu}$) and from nuclear exportation ($Whi5_{NE}$), as well as the nuclear Whi5 concentration at Start ($Whi5_{Start}$) (Figures 4B, 4C, and S4A). First, it was evident that $Whi5_{Start}$ increases as the environmental conditions worsen (Figure 4C, pink bars). This result is consistent with a recent finding that cells grown in poor nutrient had higher SBF concentration in G1 (Dorsey et al., 2018), as higher SBF implies higher Whi5 at Start. Second, we found that the absolute dilution contribution was larger in poorer conditions (Figure 4C, blue bars). This may explain why Whi5 dilution had only been previously reported in ethanol. Overall, these quantities seemed to scale with $Whi5_{peak}$.

In Figure 4D, we plot $Whi5_{dilu}$, $Whi5_{NE}$, and $Whi5_{Start}$, all normalized by $Whi5_{peak}$, versus the doubling time T_D. The data suggest that these quantities are functions of the doubling time only, just as $Whi5_{peak}$. In particular, $Whi5_{dilu}/Whi5_{peak}$ has a linear dependence on T_D, whereby $Whi5_{dilu}/Whi5_{peak} \approx aT_D + b$. Note that the rate of dilution is directly coupled to the growth rate, so this linear dependence would imply a relationship between the G1 duration T_{G1} and the doubling time T_D: $T_{G1} = (T_D/ln2) \cdot ln(1/1 - Whi5_{dilu}/Whi5_{peak}) = (T_D/ln2) \cdot ln(1/1 - aT_D - b)$, which is consistent with the experimental results (Figure S4C).

A Mathematical Model of Start Encompassing the Multiple Factors Consistently Produces All the Observed Phenomena

To further understand the dependence of $Whi5_{dilu}$, $Whi5_{NE}$, and $Whi5_{Start}$ on the doubling time, we constructed a mathematical model of the Start circuitry (Figures S4D–S4I). As illustrated in Figure 4E, the model predicted a bifurcation (initiation of the Start) as the cell grows in size. Starting from $Whi5_{peak}$ (Figure 4E, red dot), the decrease of $Whi5_{nuc}$ (Figure 4E, red line) came from two contributions: dilution due to cell growth (Figure 4E, blue

dashed line) and phosphorylation by Cdk1 (Figure 4E, the difference between the blue and red lines). The Start transition begins when $Whi5_{nuc}$ drops to the critical point (Figure 4E, black dot). The amount of these two contributions for Start, as well as the Whi5 concentration at the critical point, can be calculated (Figure 4E, blue, green, and red bars). These quantities depend on the doubling time, as schematically shown in Figure 4E, in which two sets of illustrations (dark and light colors) are presented for two doubling times.

To obtain the dependence of $Whi5_{dilu}$, $Whi5_{NE}$, and $Whi5_{Start}$ on the doubling time, we used the experimentally observed linear dependence between $Whi5_{dilu}/Whi5_{peak}$ and T_D in the model as a constraint. This resulted in a bifurcation curve uniquely determined by doubling time, so that $Whi5_{dilu}/Whi5_{peak}$, $Whi5_{NE}/Whi5_{peak}$, and $Whi5_{Start}/Whi5_{peak}$ can be determined as a function of T_D (Figure 4D, solid lines; see also STAR Methods). The excellent fit to the experimental data highlights doubling time as the most relevant single parameter characterizing the coordination of the Start.

DISCUSSION

In this work, we sought to determine how cells evaluate environmental conditions to make a reliable decision to divide. We monitored multiple rounds of cell division for single yeast cells under a variety of nutrient and stress conditions. Our work revealed a novel and elegant mechanism whereby the yeast cell sets the optimal timing for cell cycle commitment using past environmental information. That is, the level of the cell cycle inhibitor Whi5 codes the environmental condition of the past cycle(s) (Figure 1C), which in turn affects the timing of starting the current cycle (Figures 3B and S3A). Remarkably, this coding of past environmental information is just the (past) doubling time (Figure 2A). In other words, yeast cell uses its doubling time as a measure of the environmental condition and stores this information in the level of Whi5.

As outlined in the Introduction, it has long been studied how cells sense the environment and use the information to regulate cell cycle entry. However, most previous studies focused on how cells respond to the current environment, i.e., the condition in the current G1 phase. We found that Whi5, being a stable protein, can store information of the past, and this memory is used to regulate the current cell cycle entry. A combination of past memory with the assessment of current condition could optimize the cell's response and adaptation to a fluctuating environment.

To see how cell integrates past and current information, we investigated how the multiple mechanisms of triggering Start—dilution of nuclear Whi5 concentration via growth, exclusion of nuclear Whi5 via phosphorylation, and the value of Whi5 threshold at Start—coordinate in various environmental conditions. Recent work reached conflicting conclusions about whether there is growth-dependent nuclear Whi5 dilution in G1 (Dorsey et al., 2018; Schmoller et al., 2015). By studying a variety of different conditions, our work confirmed that there is growth-dependent nuclear Whi5 dilution, but its extent depends on the environment. As the environment worsens (longer doubling time), Whi5 dilution contributes more and Whi5 nuclear exportation contributes less to decreasing the Whi5 concentration in the nucleus (Figure 4D). Because cells grow more slowly in worse conditions, the greater contribution of Whi5 dilution requires a longer G1 phase for cell growth. Moreover, the G1 duration in various environments is also fine-tuned by the Start threshold of the nuclear Whi5 concentration, which increases with the doubling time (Figure 4D). One possibility for a higher Whi5 threshold in poorer conditions is a higher SBF level, which is consistent with recent observation that SBF was upregulated in the poor nutrient glycerol (Dorsey et al., 2018).

Our results show that, in a stable environment, Whi5 records the condition and contributes in the homeostasis of growth and division. We have tested whether this Whi5 "memory" would affect the cell's ability to adapt to a rapidly changing environment. We cultured cells in a poor medium (ethanol) to steady state and then shifted the medium to glucose (a rich medium). We observed that, for the next G1 phase right after the medium shift, the cell still had almost the same level of Whi5 as before (Figure S3F), so the memory was there. However, the new G1 length quickly approached the value corresponding to the new environment (Figures S3G–S3J; Data S3). This fast adaptation of G1 length is due to the other regulations in G1, which act in short timescales. There are two factors together setting the G1 length: Whi5 level (largely inherited from the previous cycle) and the environment in G1 (growth rate/Whi5 dilution rate and the nutrient condition). As can be seen from Figure 3B, even with the same Whi5 level, the G1 durations can be very different under different environments. Although Whi5 records the past, the cell also uses the current environmental information to adapt to the changing environment. In a sense, it is "anticipation" versus "adaptation." In the ethanol to glucose media shift experiment, the environmental difference was huge and "adaptation" was more dominating. On the other hand, without any environmental change (steady-state condition) or with small changes, there is no or little "adaptation," and in this case, "anticipation" plays a more important role to coordinate cell growth and division.

It was previously suggested that Whi5 can play a role in cell size control. Specifically, it was found that, under a fixed nutrient condition, a cell born smaller has higher concentration of Whi5, thus having a longer G1 phase to grow bigger (Schmoller et al., 2015). Our experiments here recapitulate all the key aspects of this model. We found that Whi5 is a stable protein, diluted in G1 and synthesized in S/G2/M. Although the model from Schmoller et al. describes how cell growth drives cell division in one particular condition, it does not aim to address or explain how different size set points can be obtained in different environmental conditions. Here, we found that, across different environmental conditions, the change in cell size is insufficient to cause the observed change in the Whi5 concentration (Figures S1H and S1I). It is possible that the yeast cells employ multiple and different size control mechanisms within and across environmental conditions to modulate their target size.

Finally, we have tried to interrogate the molecular mechanism for the observed linear correlation between Whi5 level and the doubling time across various environmental conditions (Figure 2A). We found that Whi5 protein essentially does not degrade in the cell (Figure 2B) and the Whi5 synthesis rate is approximately the same across the environmental conditions

(Figure 2C). It was previously found that, in a fixed condition (ethanol), Whi5 synthesis rate is independent of cell size (Schmoller et al., 2015). Our results reveal a constant Whi5 synthesis rate independent of both cell size and the environmental conditions (Figure S2B). In light of our finding that the number of WHI5 mRNAs is independent of the environmental conditions (Figures 2D and 2E), it is conceivable that an environmentally independent protein synthesis rate could be achieved by ribosome saturating the WHI5 mRNA.

In summary, our work revealed that, as the gate keeper of cell cycle entry, Whi5 plays a key role in coordinating cell growth and division in response to different environmental conditions. It records the past environmental information, and this is achieved in a simple and perhaps the most sensible way. On timescales of the doubling time or longer, the thing that matters the most about the environmental condition is the growth rate, which is precisely what Whi5 remembered. On shorter timescales within G1, the timing of the Start transition is further fine-tuned by the threshold of Whi5 concentration at Start and the integration of Cdk1 activity, as well as by the growth rate (dilution rate), all of which depends on the current condition. The combination of these strategies on different timescales works together to ensure an adaptive cell cycle entry.

STAR★METHODS

Detailed methods are provided in the online version of this paper and include the following:

- KEY RESOURCES TABLE
- LEAD CONTACT AND MATERIALS AVAILABILITY
- EXPERIMENTAL MODEL AND SUBJECT DETAILS
- METHOD DETAILS
  - Use of a microfluidics device
  - Time-lapse microscopy and image analysis
  - Whi5 immunoblot
  - Comparison of the Whi5 measurements using two methods
  - smFISH and imaging
  - Model construction
- MODEL PREDICTION OF $WHI5_{DILU}$ AND $WHI5_{NE}$ AS FUNCTIONS OF DOUBLING TIME
- QUANTIFICATION AND STATISTICAL ANALYSIS
  - Whi5 synthesis rate estimation
  - Quantification of Whi5 dilution and Whi5 nuclear exportation at the Start point
- DATA AND CODE AVAILABILITY

SUPPLEMENTAL INFORMATION

Supplemental Information can be found online at https://doi.org/10.1016/j.celrep.2019.09.030.

ACKNOWLEDGMENTS

We thank Yihan Lin for helpful discussions. We thank Tanqiu Liu, Zijian Zhang, and Haoyuan Sun for image analysis. This work was supported by the Ministry of Science and Technology of China (2015CB910300 and The National Key Research and Development Program of China: 2018YFA0900700) and the National Natural Science Foundation of China (NSFC31700733).

AUTHOR CONTRIBUTIONS

C.T. and Y.Q. designed the project. Y.Q. and J.J. designed and performed the experiments. Y.Q., J.J., and X.L. analyzed the data. X.L. constructed the mathematical model and performed the simulation. C.T. and X.Y. supervised the whole project; Y.Q., J.J., X.L., C.T., and X.Y. wrote the paper.

DECLARATION OF INTERESTS

The authors declare no competing interests.

Received: February 25, 2019
Revised: April 28, 2019
Accepted: September 11, 2019
Published: October 22, 2019

REFERENCES

Amigoni, L., Colombo, S., Belotti, F., Alberghina, L., and Martegani, E. (2015). The transcription factor Swi4 is target for PKA regulation of cell size at the G1 to S transition in Saccharomyces cerevisiae. Cell Cycle *14*, 2429–2438.

Arava, Y., Wang, Y., Storey, J.D., Liu, C.L., Brown, P.O., and Herschlag, D. (2003). Genome-wide analysis of mRNA translation profiles in Saccharomyces cerevisiae. Proc. Natl. Acad. Sci. USA *100*, 3889–3894.

Baroni, M.D., Monti, P., and Alberghina, L. (1994). Repression of growth-regulated G1 cyclin expression by cyclic AMP in budding yeast. Nature *371*, 339–342.

Bean, J.M., Siggia, E.D., and Cross, F.R. (2006). Coherence and timing of cell cycle start examined at single-cell resolution. Mol. Cell *21*, 3–14.

Bishop, A.C., Ubersax, J.A., Petsch, D.T., Matheos, D.P., Gray, N.S., Blethrow, J., Shimizu, E., Tsien, J.Z., Schultz, P.G., Rose, M.D., et al. (2000). A chemical switch for inhibitor-sensitive alleles of any protein kinase. Nature *407*, 395–401.

Cai, Y., and Futcher, B. (2013). Effects of the yeast RNA-binding protein Whi3 on the half-life and abundance of CLN3 mRNA and other targets. PLoS ONE *8*, e84630.

Chandler-Brown, D., Schmoller, K.M., Winetraub, Y., and Skotheim, J.M. (2017). The adder phenomenon emerges from independent control of pre- and post-start phases of the budding yeast cell cycle. Curr. Biol. *27*, 2774–2783.e3.

Costanzo, M., Nishikawa, J.L., Tang, X., Millman, J.S., Schub, O., Breitkreuz, K., Dewar, D., Rupes, I., Andrews, B., and Tyers, M. (2004). CDK activity antagonizes Whi5, an inhibitor of G1/S transcription in yeast. Cell *117*, 899–913.

Cross, F.R., and Blake, C.M. (1993). The yeast Cln3 protein is an unstable activator of Cdc28. Mol. Cell. Biol. *13*, 3266–3271.

de Bruin, R.A., McDonald, W.H., Kalashnikova, T.I., Yates, J., 3rd, and Wittenberg, C. (2004). Cln3 activates G1-specific transcription via phosphorylation of the SBF bound repressor Whi5. Cell *117*, 887–898.

Dorsey, S., Tollis, S., Cheng, J., Black, L., Notley, S., Tyers, M., and Royer, C.A. (2018). G1/S transcription factor copy number is a growth-dependent determinant of cell cycle commitment in yeast. Cell Syst. *6*, 539–554.e11.

Hall, D.D., Markwardt, D.D., Parviz, F., and Heideman, W. (1998). Regulation of the Cln3-Cdc28 kinase by cAMP in Saccharomyces cerevisiae. EMBO J. *17*, 4370–4378.

Hartwell, L.H., Culotti, J., Pringle, J.R., and Reid, B.J. (1974). Genetic control of the cell division cycle in yeast. Science *183*, 46–51.

Huh, W.K., Falvo, J.V., Gerke, L.C., Carroll, A.S., Howson, R.W., Weissman, J.S., and O'Shea, E.K. (2003). Global analysis of protein localization in budding yeast. Nature *425*, 686–691.

Johnson, A., and Skotheim, J.M. (2013). Start and the restriction point. Curr. Opin. Cell Biol. *25*, 717–723.

Jorgensen, P., and Tyers, M. (2004). How cells coordinate growth and division. Curr. Biol. *14*, R1014–R1027.

Jorgensen, P., Edgington, N.P., Schneider, B.L., Rupes, I., Tyers, M., and Futcher, B. (2007). The size of the nucleus increases as yeast cells grow. Mol. Biol. Cell *18*, 3523–3532.

Liku, M.E., Nguyen, V.Q., Rosales, A.W., Irie, K., and Li, J.J. (2005). CDK phosphorylation of a novel NLS-NES module distributed between two subunits of the Mcm2-7 complex prevents chromosomal rereplication. Mol. Biol. Cell *16*, 5026–5039.

Liu, X., Wang, X., Yang, X., Liu, S., Jiang, L., Qu, Y., Hu, L., Ouyang, Q., and Tang, C. (2015). Reliable cell cycle commitment in budding yeast is ensured by signal integration. eLife *4*, e03977.

Longtine, M.S., McKenzie, A., 3rd, Demarini, D.J., Shah, N.G., Wach, A., Brachat, A., Philippsen, P., and Pringle, J.R. (1998). Additional modules for versatile and economical PCR-based gene deletion and modification in Saccharomyces cerevisiae. Yeast *14*, 953–961.

McInerny, C.J., Partridge, J.F., Mikesell, G.E., Creemer, D.P., and Breeden, L.L. (1997). A novel Mcm1-dependent element in the SWI4, CLN3, CDC6, and CDC47 promoters activates M/G1-specific transcription. Genes Dev. *11*, 1277–1288.

Papagiannakis, A., Niebel, B., Wit, E.C., and Heinemann, M. (2017). Autonomous metabolic oscillations robustly gate the early and late cell cycle. Mol. Cell *65*, 285–295.

Polymenis, M., and Schmidt, E.V. (1997). Coupling of cell division to cell growth by translational control of the G1 cyclin CLN3 in yeast. Genes Dev. *11*, 2522–2531.

Pramila, T., Wu, W., Miles, S., Noble, W.S., and Breeden, L.L. (2006). The Forkhead transcription factor Hcm1 regulates chromosome segregation genes and fills the S-phase gap in the transcriptional circuitry of the cell cycle. Genes Dev. *20*, 2266–2278.

Raj, A., van den Bogaard, P., Rifkin, S.A., van Oudenaarden, A., and Tyagi, S. (2008). Imaging individual mRNA molecules using multiple singly labeled probes. Nat. Methods *5*, 877–879.

Schmoller, K.M., Turner, J.J., Kõivomägi, M., and Skotheim, J.M. (2015). Dilution of the cell cycle inhibitor Whi5 controls budding-yeast cell size. Nature *526*, 268–272.

Schneider, B.L., Zhang, J., Markwardt, J., Tokiwa, G., Volpe, T., Honey, S., and Futcher, B. (2004). Growth rate and cell size modulate the synthesis of, and requirement for, G1-phase cyclins at start. Mol. Cell. Biol. *24*, 10802–10813.

Shi, L., and Tu, B.P. (2013). Acetyl-CoA induces transcription of the key G1 cyclin CLN3 to promote entry into the cell division cycle in Saccharomyces cerevisiae. Proc. Natl. Acad. Sci. USA *110*, 7318–7323.

Tokiwa, G., Tyers, M., Volpe, T., and Futcher, B. (1994). Inhibition of G1 cyclin activity by the Ras/cAMP pathway in yeast. Nature *371*, 342–345.

Trcek, T., Chao, J.A., Larson, D.R., Park, H.Y., Zenklusen, D., Shenoy, S.M., and Singer, R.H. (2012). Single-mRNA counting using fluorescent in situ hybridization in budding yeast. Nat. Protoc. *7*, 408–419.

Tyers, M., Tokiwa, G., Nash, R., and Futcher, B. (1992). The Cln3-Cdc28 kinase complex of S. cerevisiae is regulated by proteolysis and phosphorylation. EMBO J. *11*, 1773–1784.

Yaglom, J., Linskens, M.H., Sadis, S., Rubin, D.M., Futcher, B., and Finley, D. (1995). p34Cdc28-mediated control of Cln3 cyclin degradation. Mol. Cell. Biol. *15*, 731–741.

Yang, X., Lau, K.Y., Sevim, V., and Tang, C. (2013). Design principles of the yeast G1/S switch. PLoS Biol. *11*, e1001673.

Zhang, Z.B., Wang, Q.Y., Ke, Y.X., Liu, S.Y., Ju, J.Q., Lim, W.A., Tang, C., and Wei, P. (2017). Design of tunable oscillatory dynamics in a synthetic NF-κB signaling circuit. Cell Syst. *5*, 460–470.e5.

STAR★METHODS

KEY RESOURCES TABLE

REAGENT or RESOURCE	SOURCE	IDENTIFIER
Antibodies		
anti-FLAG antibody	CST	Cat# 8146, RRID: AB_10950495
anti-α-tubulin antibody	MBL	Cat# PM054, RRID: AB_10598496
anti-mouse IgG	LI-COR	Cat# C50721-02
anti-rabbit IgG	LI-COR	Cat# C50618-03
Experimental Models: Organisms/Strains		
W303 (MATa leu2-3/112 ura3-1 trp161 his3-11/15 can1-100 GAL SUC2 mal0)	Gift from Ping Wei	N/A
JAU01 (W303 cdc28-as1)	Bishop et al., 2000	N/A
QYJS002 (W303 WHI5-tdTomato::URA3)	This study	N/A
QYJS008 (W303 WHI5-8FLAG::kanMX)	This study	N/A
QYMS009 (W303 WHI5-tdTomato::URA3 WHI5pr-ORF-tdTomato::HIS3)	This study	N/A
QYMS010 (W303 WHI5-tdTomato::URA3 WHI5pr-ORF-tdTomato::HIS3 WHI5pr-ORF-tdTomato::TRP1)	This study	N/A
QYMS012 (W303 WHI5::NAT ADH1pr-MCM-GFP::HIS3)	This study	N/A
QYMS013 (W303 WHI5-tdTomato::URA3 ADH1pr-MCM-GFP::HIS3)	This study	N/A
Recombinant DNA		
pFA6-KAN-MX6	Longtine et al., 1998	N/A
pNI8-WHI5-tdTomato-CaURA3	Liu et al., 2015	N/A
pNH603-ADH1pr	Gift from Ping Wei	N/A
pZeroback-8FLAG-KANMX	This study	N/A

LEAD CONTACT AND MATERIALS AVAILABILITY

Further information and requests for resources and reagents should be directed to and will be fulfilled by the Lead Contact, Chao Tang (tangc@pku.edu.cn) and Xiaojing Yang (xiaojing_yang@pku.edu.cn).

All unique reagents generated in this study are available from the Lead Contact without restriction.

EXPERIMENTAL MODEL AND SUBJECT DETAILS

All the strains used in this study were congenic *W303*. Standard protocols were used throughout. The plasmids were replicated in DH5α *Escherichia coli*. All constructs were confirmed by both colony PCR and sequencing.

Whi5 was tagged with the fluorescent protein tdTomato at its C terminus and expressed from its endogenous locus. The Whi5-tdTomato strain (QYJS002) was constructed by transformation of the pNI8-WHI5-tdTomato-CaURA3 plasmid, which was composed of the following elements: $WHI5_{(385-888)}$-tdTomato-TEF1 terminator-TEF1 promoter-CaURA3-TEF1 terminator-312 bp of WHI5 gene downstream (Liu et al., 2015). The plasmids were digested with HindIII to release the entire cassette for integration. Eight copies of FLAG were integrated into the endogenous WHI5 gene locus by using PCR products from pNI8-WHI5-tdTomato-CaURA3 plasmid to make the strain (QYJS008). The pZeroback-8FLAG-KANMX plasmid was constructed based on the pZeroback backbone (VT131112, TIANGEN Biotech (Beijing) Co., Ltd.).

Mediums used for yeast culture are shown in Data S1. For imaging, single colonies were picked from YPAD agar plates and dispensed into 3∼4 mL of relative media. Detailed medium information is listed in Data S3. Cells were then grown at 30°C overnight in a shaking incubator. The overnight cultures were diluted to an OD_{600} of 0.05 into 4ml of relative media. Cells were grown to an OD_{600} of 0.5 for imaging.

METHOD DETAILS

Use of a microfluidics device

The microfluidics device was constructed with polydimethylsiloxane using standard techniques of soft lithography and replica molding (Figure S1A). The cells were quickly concentrated and loaded into the microfluidics device. A syringe filled with 1ml medium was connected to the inlet using soft polyethylene tubing. The flow of medium into the chip was maintained by an auto-controlled syringe pump (TS-1B, Longer Pump Corp., Baoding, China) with a constant velocity of 66.7 μl/hour. The microfluidics system was maintained at 30°C to avoid introducing air bubbles and for yeast growth. Cells were precultured for 2 hr in the microfluidics chip before imaging.

Time-lapse microscopy and image analysis

All images were captured by a Nikon Observer microscope with an automated stage and Perfect-Focus-System (Nikon Co., Tokyo, Japan) using an Apo 100 × /1.49 oil TIRF objective. We used filter sets that are optimized for the detection of Whi5-tdTomato fluorescent protein and acquired images at 3-minute intervals. The exposure time is 100ms. Cell segmentation and fluorescent quantification were performed by Cellseg. By cell segmentation, every pixel of the cell could be quantified in the fluorescence channel. $Whi5_{peak}$ was used to compare the maximum nuclear concentration of Whi5 ($Whi5_{nuc}$) in G1 phase under different environmental conditions. As Whi5 localizes in the nucleus in G1 phase (Figure S1B), we used the mean intensity of the brightest 5 × 5 Whi5-tdTomato pixels in one cell to estimate the nuclear concentration of Whi5in G1 phase. As previously described (Liu et al., 2015), both the intensity and the dynamics of Whi5 in the nucleus can be well represented by using the brightest 5 × 5 Whi5-tdTomato pixels (Figure SS5 in Liu et al., 2015). $Whi5_{peak}$ is the maximum of $Whi5_{nuc}$ during a G1 phase. The G1 duration was taken as the time lapse between the maximum and minimum of the first derivative of $Whi5_{nuc}$ (Figures 1A and S1) (Liu et al., 2015; Papagiannakis et al., 2017). The doubling time was defined as the time interval between two adjacent entrances of Whi5. We used the MCM marker (Liku et al., 2005; Yang et al., 2013) to quantify the G1 duration of *whi5Δ* strains and wild-type strains (Data S3) in the media-shift experiments (Figures S2D–S2H). We used the mean intensity of the brightest 5 × 5 MCM-GFP pixels in one cell to estimate the nuclear concentration of MCM in G1 phase. The G1 duration was taken as the time lapse between the maximum and minimum of the first derivative of the nuclear concentration of MCM.

Whi5 immunoblot

Strain QYS7008 (W303 *WHI5::WHI5-8FLAG::kanMX*) was generated using the pZeroback-8FLAG-KANMX plasmid. Cells were grown at 30°C to mid-log phase (OD_{600nm} = 0.5) in the corresponding media. Then, 15 mL samples were removed at relative time intervals from corresponding media, pelleted and immediately frozen in liquid nitrogen. Frozen cells were resuspended in 200 μL lysis buffer (0.1 M NaOH, 0.05 M EDTA, 2% SDS and 2% β-mercaptoethanol) and heated at 90°C for 10 min. Next, 5 μL of 4 M acetic acid were added to the lysates, vortexed for 30 s and heated at 90°C for another 10 min. Then, 50 μL of loading buffer were added to samples, which were centrifuged for 10min at 13,000 g; 20 μL of each sample was run on a SDS-PAGE. The gels were cut to include only the relevant molecular weight range, and proteins from all gels were transferred to a PVDF (polyvinylidene fluoride) membrane using a Bio Rad transfer device overnight at 4°C. The membranes were blocked for 1 hr at room temperature (~25°C). The membranes were incubated with 1:1000 mouse monoclonal anti-FLAG antibody (8146; CST) and rabbit anti-α-tubulin antibody (PM054; MBL) diluted in blocking buffer at room temperature for 1hr. Then, the membranes were washed 6 times in TBST buffer (TBS including 0.1% Tween-20). The PVDF membrane with the anti-FLAG and anti-α-tubulin antibody were then incubated with 1:10000 anti-mouse IgG (C50721-02; LI-COR) and anti-rabbit IgG (C50618-03; LI-COR) secondary antibodies at room temperature for 1hr before being washed 3 times in TBST and 2 times in PBS. Finally, the membranes were imaged using a fluorescent imager (LI-COR; Odyssey CLx Imager).

Comparison of the Whi5 measurements using two methods

To test whether the intensity of fluorescent proteins differ systematically between media conditions, we compared the GFP intensity of the endogenously tagged GFP to immunofluorescence against this tag in different conditions (Glc, Eth and NaCl). We deployed a doxycycline-induced GFP strain (Zhang et al., 2017), cultured it in different conditions, and induced GFP expression by adding 50 g/ml doxycycline. After 2h induction, we immunostained the cells with the anti-GFP antibody (CST, 2956) and Goat Anti-Rabbit IgG (Abcam, ab150088), and used FACS to measure the GFP intensity and PE 594 intensity. We used the culture without addition of doxycycline as the control. We found that the GFP intensity and immunofluorescence intensity showed similar results in all three different environmental conditions we tested (Figure S1K).

smFISH and imaging

Single-molecule FISH of *WHI5* mRNA was performed as described in Trcek et al. (2012). The numbers of mRNA molecules were determined from a maximal projection of 30 5-μm z stacks. We detected single mRNAs based on previously described methods (Raj et al., 2008). We used A594 as the fluorescent probe (Thermo Fisher Scientific).

Model construction

We constructed a mathematical model to explain the theoretical analysis of the positive feedback loop between Whi5 and Cln1/2 and assess the contributions of different factors on the bistability of nuclear Whi5 (Figures S4E and S4F).

For simplicity, we used c to denote the concentration of nuclear Cln1/2, w_{in} and w_t to denote nuclear Whi5 concentration ($Whi5_{nuc}$) and whole cell Whi5 concentration ($Whi5_{total}$). We also considered SBF, denoting the free active SBF as s_f concentration and the total nuclear concentration of SBF as s_t.The equations used were as follows:

$$\begin{cases} \dfrac{dc}{dt} = V_{12}\dfrac{s_f^{n_1}}{K_s^{n_1}+s_f^{n_1}} - D_{12}c \\ s_f = g(s_t, w_{in}) = \dfrac{2K_D s_t}{K_D + w_{in} - s_t + \sqrt{(K_D + w_{in} - s_t)^2 + 4K_D s_t}} \\ \quad = \dfrac{2s_t}{1 + \dfrac{w_{in}}{K_D} - \dfrac{s_t}{K_D} + \sqrt{\left(1 + \dfrac{w_{in}}{K_D} - \dfrac{s_t}{K_D}\right)^2 + 4\dfrac{s_t}{K_D}}} \\ \dfrac{dw_{in}}{dt} = -v\dfrac{c^{n_2}}{K_c^{n_2}+c^{n_2}}w_{in} + p(w_t - w_{in}) \end{cases} \quad \text{(s1.1)},$$

Note that the deduction of s_f, denoted as the function g, is shown below.

To nondimensionalize this model, we applied the following substitutions:

$$\tau = D_{12}t$$

$$\tilde{c} = \frac{D_{12}}{V_{12}}c$$

$$\tilde{w}_{in} = \frac{w_{in}}{K_D}$$

$$\tilde{s}_f = \frac{s_f}{K_D}, \tilde{s}_t = \frac{s_t}{K_D}, \tilde{w}_t = \frac{w_t}{K_D}, \tilde{K}_s = \frac{K_s}{K_D}, \tilde{K}_c = \frac{D_{12}K_c}{V_{12}}, A = \frac{v}{D_{12}}$$

Finally, we arrived

$$\begin{cases} \dfrac{d\tilde{c}}{d\tau} = \dfrac{\tilde{s}_f^{n_1}}{\tilde{K}_s^{n_1}+\tilde{s}_f^{n_1}} - \tilde{c} \\ \tilde{s}_f = \dfrac{g(s_t, w_{in})}{K_D} = \dfrac{2\tilde{s}_t}{1 + \tilde{w}_{in} - \tilde{s}_t + \sqrt{(1 + \tilde{w}_{in} - \tilde{s}_t)^2 + 4\tilde{s}_t}} \\ \dfrac{d\tilde{w}_{in}}{d\tau} = A\left[-\dfrac{\tilde{c}^{n_2}}{\tilde{K}_c^{n_2}+\tilde{c}^{n_2}}\tilde{w}_{in} + \dfrac{p}{v}(\tilde{w}_t - \tilde{w}_{in})\right] \end{cases} \quad \text{(s1.2)}$$

To show the bistability of this system clearly, we calculated the nullclines (Figure S4G) as follows:

$$\tilde{c} = \frac{\tilde{s}_f^{n_1}}{\tilde{K}_s^{n_1}+\tilde{s}_f^{n_1}} \quad \text{(s1.3)}$$

$$\tilde{w}_{in} = \tilde{w}_t\left(1 - \frac{v}{p+v}\frac{\tilde{c}^{n_2}}{\frac{p}{p+v}\tilde{K}_c^{n_2}+\tilde{c}^{n_2}}\right) \quad \text{(s1.4)}.$$

By changing the values of $\tilde{w}_t$ and $\tilde{s}_t$, the nullclines change as well, and the system comes to a saddle-node bifurcation. Once the bifurcation occurs, the high steady-state vanishes and the nuclear whi5 concentration drops to a lower level. To clearly show how the total Whi5 and SBF concentrations influence this bifurcation, we chose one set of parameters and showed their bifurcation plot (Figures S4G–S4I). In Figure S4G, we show the bifurcation plot of $Whi5_{nuc}$ versus cell size. We use $(C/\tilde{w}_t)$ to represent cell size for the product of cell size and C as a constant during G1 phase.

We can also introduce Cln3 into this model by changing (dw_{in}/dt) to

$$\frac{dw_{in}}{dt} = -v\frac{c^{n_2}}{K_c^{n_2}+c^{n_2}}w_{in} - v_3\frac{c_3^{n_3}}{K_{c3}^{n_3}+c_3^{n_3}}w_{in} + p(w_t - w_{in}) \quad \text{(s1.6)}$$

After the nondimensionalization, we have

$$\frac{d\tilde{w}_{in}}{d\tau} = A\left[-\frac{\tilde{c}^{n_2}}{\tilde{K}_c^{n_2}+\tilde{c}^{n_2}}\tilde{w}_{in} - C_3\tilde{w}_{in} + \frac{p}{v}(\tilde{w}_t - \tilde{w}_{in})\right] \quad \text{(s1.5)},$$

where

$$C_3 = \frac{v_3}{v}\frac{c_3^{n_3}}{K_{c3}^{n_3}+c_3^{n_3}}.$$

Since C_3 is positively associated with the Cln3 expression level, we just used C_3 to show the contribution of Cln3. In the same way, we analyzed the role of Cln3 in bistability and showed the bifurcation plot (Figure S4H).

In the end we deduced function g.Here we assumed that the inhibition of SBF by nuclear Whi5 was through direct binding and both Whi5 and SBF have finite concentrations. Thus, we had the following equations (K_D is the dissociation constant):

$$SBF^f + \mathrm{Whi5}_{\mathrm{in}}^f \leftrightarrow [SBF \cdot Whi5_{in}]$$

$$SBF^f + [SBF \cdot Whi5_{in}] = SBF^t$$

$$Whi5_{in}^f + [SBF \cdot Whi5_{in}] = Whi5_{in}$$

Then, we obtained

$$s_f = g(s_t, w_{in}) = \frac{2K_D s_t}{K_D + w_{in} - s_t + \sqrt{(K_D + w_{in} - s_t)^2 + 4K_D s_t}}$$

Using the model above, we developed a method for identifying the Whi5 nuclear expression level at the Start point defined in the experiment $(\mathrm{Whi5}_s^{nuc})$. The specific method is that for a given set of parameters, we calculate a corresponding critical $\tilde{w}_t^c$ where bifurcation occurs. At this $\tilde{w}_t^c$, we gave the high-steady-state a perturbation and set it as the initial point for the ODE system. Through numerical simulation, the system will "jump" to a low-steady-state. During this transient state, $(d\tilde{w}_{in}/d\tau)$ achieves a maximum. The $\tilde{w}_{in}$ and corresponding w_{in} are considered to be the theoretical $\mathrm{Whi5}_s^{nuc}$ from the model.

MODEL PREDICTION OF $\mathrm{WHI5_{DILU}}$ AND $\mathrm{Whi5_{NE}}$ AS FUNCTIONS OF DOUBLING TIME

We first predicted the change of $\mathrm{Whi5_{dilu}}$ with different SBF concentration using the method above. Once we knew the relationship between $(\mathrm{Whi5_{dilu}}/\mathrm{Whi5_{peak}})$ and the doubling time (Figure 4D, blue dots), we could derive a relationship between $\mathrm{Whi5_{dilu}}$ and the doubling time. By fitting this relationship, we predicted a theoretical relationship describing concentration of SBF change with doubling time. Then the model predicted $\mathrm{Whi5_{NE}}$ for every specific s_t(concentration of SBF). Finally, a prediction of $\mathrm{Whi5_{dilu}}$ and $\mathrm{Whi5_{NE}}$, which changed with the doubling time was made (Figure 4D, solid line). All of the parameters used in this prediction were listed in Data S4.

QUANTIFICATION AND STATISTICAL ANALYSIS

Whi5 synthesis rate estimation

To estimate Whi5 synthesis rate, we analyzed time series for the amount of Whi5–tdTomato in the cell during the S/G2/M phase of the cell cycle. This phase was determined as shown in Figure S1C. The synthesis rate of Whi5 in one cell is estimated by dividing the accumulation of the amount of Whi5 in the cell (including its bud) during the S/G2/M phase by the corresponding S/G2/M duration.

Quantification of Whi5 dilution and Whi5 nuclear exportation at the Start point

To calculate the contribution of Whi5 dilution at the Start point, we first calculated the hypothetical nuclear Whi5 concentration at Start if the change of Whi5 nuclear concentration were only due to cell growth (dilution):

$$\mathrm{Whi5_{dilu}} = \mathrm{Whi5_{peak}}\frac{V_{\mathrm{peak}}^{\mathrm{nuc}}}{V_{\mathrm{start}}^{\mathrm{nuc}}} = \mathrm{Whi5_{peak}}\frac{V_{\mathrm{peak}}}{V_{\mathrm{start}}} = \mathrm{Whi5_{peak}}\left(\frac{A_{\mathrm{peak}}}{A_{\mathrm{start}}}\right)^{3/2},$$

where $V_{\mathrm{peak}}^{\mathrm{nuc}}$ is the nuclear volume at the time when Whi5 nuclear concentration reaches its maximum value $\mathrm{Whi5_{peak}}$, $V_{\mathrm{start}}^{\mathrm{nuc}}$ is the nuclear volume at Start, V_{peak} and V_{start} are the cell volumes at the two corresponding time points, A_{peak} and A_{start} are the cell areas at the two time points, which are measured directly in the experiments. The total decrease in nuclear Whi5 concentration during G1 is $\mathrm{Whi5_{down}} = \mathrm{Whi5_{peak}} - \mathrm{Whi5_{start}}$. Thus, the decrease due to Whi5 nuclear exportation is $\mathrm{Whi5_{NE}} = \mathrm{Whi5_{down}} - \mathrm{Whi5_{dilu}}$.

DATA AND CODE AVAILABILITY

The published article contains all the datasets generated in Data S1, S2, S3, and S4.